Macrocyclic Inhibitors for Peptide Deformylase: A Structure−Activity Relationship Study of the Ring Size

Xubo Hu,[†,‡] Kiet T. Nguyen,[†,‡] Vernon C. Jiang,[§] Denene Lofland,[§] Heinz E. Moser,[§] and Dehua Pei*[,†]

Department of Chemistry and Ohio State Biochemistry Program, The Ohio State University, 100 West 18th Avenue, Columbus, Ohio 43210, and GeneSoft Pharmaceuticals Inc., 7300 Shoreline Court, South San Francisco, California 94080

Received May 28, 2004

Peptide deformylase (PDF) catalyzes the removal of the N-terminal formyl group from newly synthesized polypeptides in eubacteria. Its essential role in bacterial cells but not in mammalian cells makes it an attractive target for antibacterial drug design. We have previously reported an N-formylhydroxylamine-based, metal-chelating macrocyclic PDF inhibitor, in which the P_1' and P_3' side chains are covalently joined. In this work, we have carried out a structure−activity relationship study on the size of the macrocycle and found that 15−17-membered macrocycles are optimal for binding to the PDF active site. Unlike the acyclic compounds, which are simple competitive inhibitors, the cyclic compounds all act as slow-binding inhibitors. As compared to their acyclic counterparts, the cyclic inhibitors displayed 20−50-fold higher potency against the PDF active site (K_I* as low as 70 pM), improved selectivity toward PDF, and improved the metabolic stability in rat plasma. Some of the macrocyclic inhibitors had potent, broad spectrum antibacterial activity against clinically significant Gram-positive and Gram-negative pathogens. These results suggest that the macrocyclic scaffold provides an excellent lead for the development of a new class of antibiotics.

Introduction

Peptide deformylase (PDF) has emerged as an exciting new target for designing novel antibiotics to treat antibiotic resistant pathogens.[1−4] PDF is an essential enzyme involved in bacterial protein biosynthesis and maturation. In bacteria and the organelles of eukaryotes, protein synthesis starts with an N-formylmethionine, and as a result, all newly synthesized polypeptides carry transiently a formylated N terminus.[5] PDF catalyzes the subsequent removal of the formyl group from the vast majority of those polypeptides, many of which undergo further N-terminal processing by methionine aminopeptidase to produce mature proteins. PDF is present in all eubacteria, and its essentiality for bacterial survival has been demonstrated by both genetic studies[6−8] and arrest of bacterial growth by PDF inhibitors.[1−4] On the other hand, protein synthesis in the eukaryotic cytoplasm does not involve N-terminal formylation, and PDF apparently has no catalytic function in the mammalian mitochondrion.[9] Furthermore, PDF is a metallopeptidase that contains a tetrahedrally coordinated, catalytically essential ferrous ion (Fe^{2+}) in the active site.[10,11] These properties make PDF an attractive antibacterial drug target.

Numerous PDF inhibitors have been reported in recent years; essentially, all of them are metal chelators such as thiols,[12−14] hydroxamates,[15−20] and N-formylhydroxylamines or reverse hydroxamates.[21,22] Many of these inhibitors exhibit excellent antibacterial activities in vitro and in animal studies. One of the reverse hydroxamates from British Biotech, BB86398, has been advanced into clinical trials for the treatment of hospitalized community-acquired pneumonia. However, because most of these inhibitors are metal chelators appended to peptidomimetics, there remains some concern about their selectivity (e.g., inhibition of other metalloproteases) and in vivo stability (e.g., proteolysis of the peptide bonds). A popular approach to improving both stability against proteolysis and selectivity of peptidomimetic inhibitors is to form cyclic peptides or depsipeptides.[23,24] Structural studies of several PDF−inhibitor complexes[21,25,26] have revealed that the inhibitors are bound in an extended conformation and the P_1' and P_3' side chains are similarly oriented. While the P_2' side chain is extended toward solvent, the P_1' and P_3' side chains are engaged in intimate interactions with the enzyme. The P_1' side chain (usually an *n*-butyl group) fits into a deep hydrophobic pocket in the PDF active site. The P_3' side chain makes hydrophobic contacts with a shallow pocket near the active site as well as one face of the P_1' side chain. We have recently reported a macrocyclic PDF inhibitor, in which the P_1' and P_3' side chains are covalently cross-linked (Figure 1, compound **1b**).[27] Compound **1b** was an exceedingly potent PDF inhibitor (apparent $K_I = 0.67$ nM) and was approximately 10-fold more potent than the acyclic counterpart **2** (BB-3497). We attributed the improved potency against the enzyme to the rigidity introduced by cyclization, which may lock the inhibitor into a PDF-binding conformation. We anticipated that the increased rigidity should also improve both selectivity and stability by preventing their binding to other enzymes (e.g., other peptidases). In this work, we report the synthesis and evaluation of a series of macrocyclic inhibitors of different ring sizes. These cyclic inhibitors show good antibacterial activity and markedly improved metabolic stability and selectivity.

* To whom correspondence should be addressed. Tel: 614-688-4068. Fax: 614-292-1532. E-mail: pei.3@osu.edu.
[†] The Ohio State University.
[‡] These two authors contributed equally to this work.
[§] Genesoft Pharmaceuticals Inc.

10.1021/jm049592c CCC: $27.50
Published on Web 08/24/2004

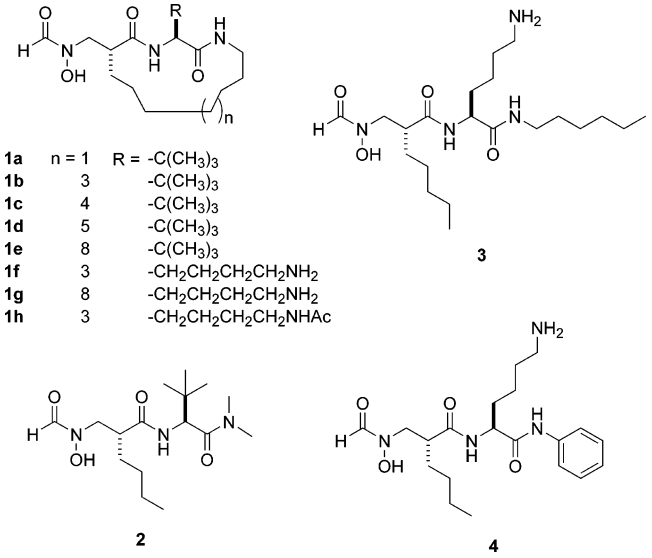

Figure 1. Structures of PDF inhibitors.

Chemistry

In the 15-membered cyclic inhibitor (Figure 1; compound **1b**) that we reported previously, the P_1' and P_3' side chains were replaced with a nonyl group.[27] Molecular modeling showed that the peptide backbone in **1b** should exist in an extended conformation. We anticipated that the ring size could greatly affect the conformation and rigidity of the peptide backbone and, therefore, the binding affinity. To determine the optimal ring size(s), we designed and synthesized compounds **1a**−**e**, which contain 13−20-membered macrocycles (Figure 1). Our attempt to form a 12-membered macrocycle ($n = 0$) failed at the olefin metathesis step, presumably due to geometric constraints in the corresponding diene. We chose *tert*-leucine as the P_2' residue in **1a**−**e** because the *tert*-butyl group is well-documented for its ability to improve both the metabolic stability and the oral bioavailability of peptidyl drugs.[21,22] However, one of the main goals for designing cyclic PDF inhibitors was to improve their in vivo stability through cyclization so that residues other than *tert*-leucine can be tolerated at the P_2' position. Because PDF has very broad specificity for the P_2' side chain,[21,25,26,28,29] this would provide an opportunity to optimize the pharmacokinetic parameters of the inhibitor by varying the P_2' structure. To test this notion, a lysine was chosen as the P_2' residue in **1f**−**h**. The lysine-containing compounds should be susceptible to proteolysis by trypsin-like proteases, thus allowing us to evaluate the effect of cyclization on the inhibitor selectivity and stability. For this reason, the open chain compounds **3** and **4** were prepared for comparison.

A convergent synthesis for the inhibitors was developed (Scheme 1). The macrocycles may be readily obtained from their diene precursors (**5**) via olefin metathesis. The dienes can be prepared by coupling the common acid **6** to the various alkenylamine **7**. The synthesis of acid **6** has been previously reported.[27] The synthesis of compounds **1a**−**e**, which contain *tert*-leucine as the P_2' residue, is illustrated in Scheme 2. The alkenykamines **8a**−**e** were prepared from the corresponding alcohols or halides. Condensation of the amines with N-Boc-*tert*-leucine followed by treatment with

Scheme 1

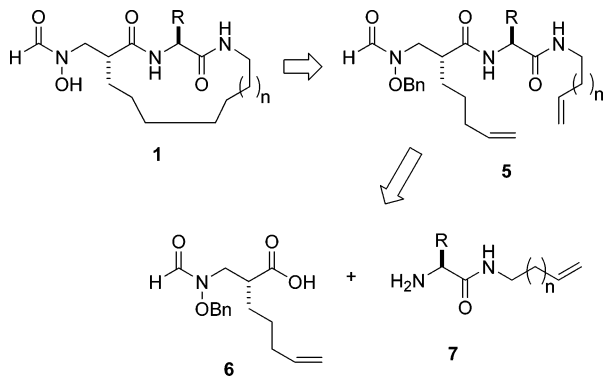

Scheme 2[a]

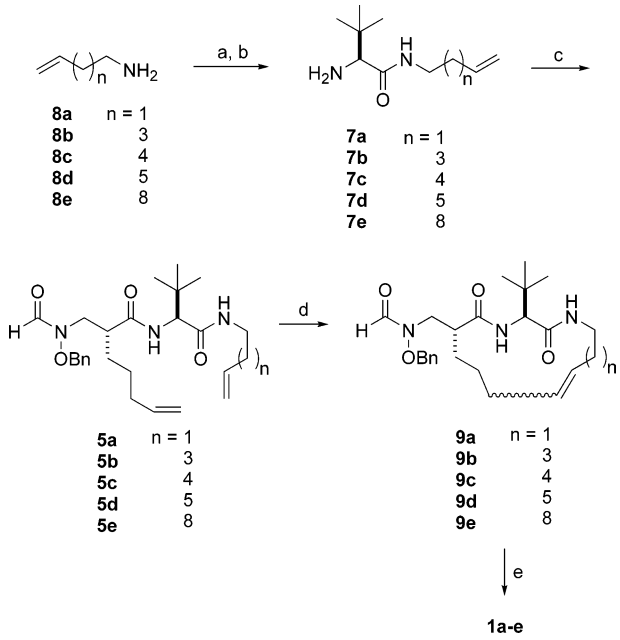

[a] Conditions: (a) Boc-*tert*-Leu-OH, EDC, CH_2Cl_2. (b) TFA. (c) Compound **6**, EDC, CH_2Cl_2. (d) $(Pcy_3)_2Cl_2Ru{=}CHPh$, CH_2Cl_2, reflux. (e) Pd/C, H_2, MeOH−EtOAc.

trifluoroacetic acid (TFA) gives the amines **7a**−**e**. The coupling of amines **7a**−**e** and acid **6** gave dienes **5a**−**e**. The terminal alkenes were cross-linked using Grubbs's ruthenium catalyst[30,31] to produce the macrocycles **9a**−**e**. Subsequent hydrogenation on Pd/C removes the benzyl group from the hydroxylamine moiety and reduces the ring carbon−carbon double bond to afford **1a**−**e**. Compounds **1f**,**g** were similarly prepared, except that N^{α}-Fmoc-N^{ϵ}-Boc-L-lysine was used instead of N-Boc-*tert*-leucine (Scheme 3). Following ring closure and hydrogenation, the Boc group was removed by treatment with TFA. Compound **1h** was obtained by reacting **1f** with acetic anhydride. Compound **3** was prepared by catalytic hydrogenation of diene **11a** and treatment with TFA (Scheme 3). Compounds **2** and **4** were synthesized as previously described.[9]

Results and Discussion

Slow-Binding Inhibition of PDF. The macrocycles **1a**−**h** were initially tested against PDF by coupling the deformylase reaction with those of formate dehydrogenase[32,33] or *Aeromonas* aminopeptidase (AAP).[34] Surprisingly, these inhibitors exhibited a slow-binding

Scheme 3[a]

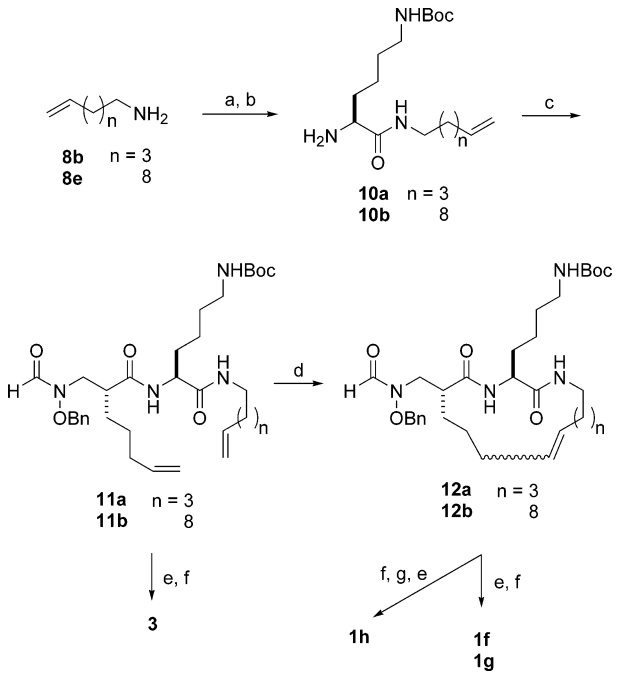

[a] Conditions: (a) Fmoc-Lys(Boc)-OH, EDC, CH_2Cl_2. (b) Piperidine, CH_2Cl_2. (c) Compound **6**, EDC, CH_2Cl_2. (d) $(Pcy_3)_2Cl_2Ru{=}CHPh$, CH_2Cl_2, reflux. (e) Pd/C, H_2, MeOH−EtOAc. (f) TFA, CH_2Cl_2. (g) Ac_2O.

behavior[35] against PDF. Coupled with their exceptional potency, a detailed kinetic characterization of the inhibitors using the above assay methods proved problematic. To this end, we recently developed a new PDF assay by coupling with dipeptidyl peptidase I (DPPI) and employing peptide f-Met-Lys-AMC as the substrate.[36] Because none of the PDF inhibitors that we have tested showed any inhibition against DPPI (DPPI is a cysteine protease), the new assay can be carried out in a continuous fashion and is ideally suited for kinetic characterization of the slow-binding inhibitors **1a**−**h**. Figure 2A shows the reaction progress curves in the absence and in the presence of inhibitor **1c**. In the absence of inhibitors, the reaction progress curve was essentially a linear line. Straight lines were also observed in the presence of competitive, acyclic inhibitors **2**−**4** (not shown). However, the cyclic inhibitors **1a**−**h** each resulted in biphasic curves. The inhibition kinetics can be described by the equation

$$E + I \underset{}{\overset{K_I}{\rightleftharpoons}} E^{\bullet}I \underset{k_6}{\overset{k_5}{\rightleftharpoons}} E^{\bullet}I^*$$

where K_I denotes the equilibrium inhibition constant of the initial enzyme−inhibitor complex ($E^{\bullet}I$) and k_5 and k_6 are the forward and reverse rate constants for the slow conversion of the initial $E^{\bullet}I$ complex into a tight-binding complex $E^{\bullet}I^*$, respectively. The overall potency of the inhibitor is described by the equilibrium constant, $K_I^* = K_I k_6/(k_5 + k_6)$. The initial inhibition constant K_I was determined by initiating the assay reactions (which contained varying concentrations of the inhibitor) by the addition of PDF and fitting the initial rates against the Michaelis−Menten equation. The K_I^* values were determined by preincubating the enzyme and various

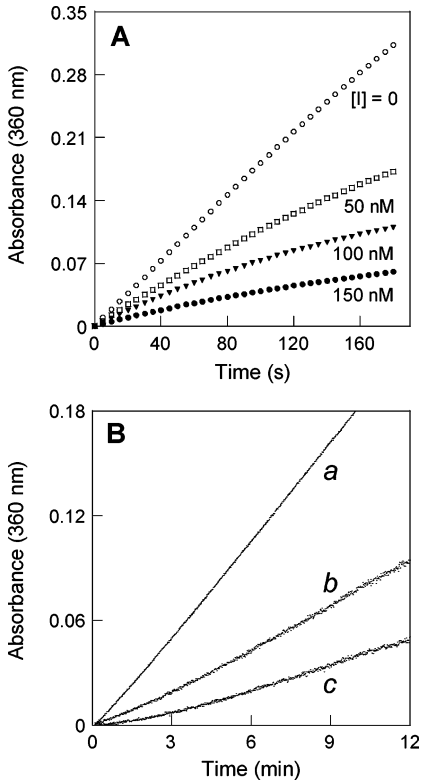

Figure 2. Slow-binding inhibition of PDF by compound **1c**. (A) Reaction progress curves when PDF was added as the last component. Each assay reaction contained buffer A, DPPI (0.1 U), f-Met-Lys-AMC (130 μM), the indicated concentration of **1c** (0, 50, 100, or 150 nM), and PDF (4.0 nM). (B) Reaction progress curves when substrate was added as the last component. PDF (100 nM) and varying concentrations of **1c** were preincubated for 2 h and rapidly diluted (10-fold) into buffer A containing f-Met-Lys-AMC (270 μM) and DPPI (0.1 U). *a*, control reaction with 1.0 nM PDF (no inhibitor); *b*, 120 nM inhibitor; and *c*, 140 nM inhibitor.

concentrations of the inhibitor for 2 h prior to the addition of substrate. To distinguish slow-binding inhibition from time-dependent irreversible inactivation and to determine the rate constant k_6, the inhibitors were preincubated with PDF to form the $E^{\bullet}I^*$ complex, which was then rapidly diluted into an assay solution containing the PDF substrate, f-Met-Lys-AMC. The slow, time-dependent recovery of PDF activity demonstrates that the inhibition is reversible and thus slow binding in nature (Figure 2B). Curve fitting gave the reactivation rate constant (k_6), in this case 0.0037 min^{-1}, for inhibitor **1c**.

Table 1 lists the inhibition constants for the tested inhibitors. All of the cyclic inhibitors exhibited a slow-binding behavior, whereas the acyclic compounds (**2**−**4**) all acted as simple competitive inhibitors under the same conditions, with K_I values of 11,[9] 74, and 23 nM, respectively. A comparison of compounds **1a**−**e**, which only differ in their ring sizes, reveals that a 15−17-membered ring (n = 6−8) is optimal for binding to the PDF active site (K_I^* = 0.22−0.33 nM against *Escherichia coli* PDF). For inhibitors of smaller (e.g., **1a**) or larger (e.g., **1e**) rings, cyclization actually slightly decreased their potency (Table 1, compare the K_I^* values of **1a**,**e** and the K_I value of **2**). Note that with the exception of the largest ring **1e**, the other four cyclic inhibitors all have similar initial K_I values (64−109 nM) to that of the acyclic control **3** (74 nM). Presumably, the

Table 1. Inhibition Constants against *E. coli* PDF

inhibitor	K_I (nM)[a]	K_I* (nM)[b]	k_5 (min^{-1})	k_6 (min^{-1})[c]
1a	63 ± 12	13.7 ± 3.0	0.022	0.0061 ± 0.0015
1b	109 ± 5	0.33 ± 0.15	1.2	0.0038 ± 0.0010
1c	96 ± 17	0.23 ± 0.06	1.6	0.0037 ± 0.0010
1d	77 ± 20	0.22 ± 0.04	0.50	0.0015 ± 0.0008
1e	2100 ± 500	25 ± 6	1.0	0.012 ± 0.0058
1f	92 ± 20	3.0 ± 1.3	0.12	0.0042 ± 0.0011
1g	258 ± 28	36 ± 9	0.11	0.018 ± 0.0045
1h	710 ± 170	12 ± 4	0.28	0.0048 ± 0.0008
2	11 ± 1	N/A[d]	N/A	N/A
3	74 ± 17	N/A	N/A	N/A
4	23 ± 6	N/A	N/A	N/A

[a] K_I values were determined by the DPPI assay in a continuous fashion. [b] K_I* values were determined by the AAP assay in the end-point format. [c] k_6 values were determined by diluting a preformed E•I* complex into a large volume of assay buffer containing f-Met-Lys-AMC and DPPI. [d] N/A, not applicable (no slow-binding behavior). All values reported represent the mean ± SD from three independent sets of experiments.

cyclic inhibitors initially bind to PDF in a manner similar to the acyclic counterpart and then undergo a slower conformational change in the inhibitor and/or protein structure. The nature of the conformational change(s) is yet unclear and will be the subject of future work. Consistent with this model, compound **1a**, which has the smallest ring size and highest rigidity, is likely more restricted from the conformational change(s) as reflected by its slow k_5 rate (0.022 min^{-1}) and similar K_I (63 nM) and K_I* values (14 nM). The greater K_I value for **1e** suggests that its larger P_1'−P_3' side chains may impede its access to the enzyme active site. Alternatively, the larger rings have more conformational flexibility; thus, a smaller fraction of the molecules has the proper preexisting conformation in the solution that can fit the contour of the PDF active site. As a result, **1e** has an overall potency similar to that of the acyclic control **3**. Cyclic inhibitors that contain an L-lysine or acetylated lysine as the P_2' residue (**1f**−**h**) are generally less potent than those containing *tert*-leucine at this position (e.g., compare **1b** vs **1f**). This is mainly due to slower conversion from E•I to E•I* (slower k_5) for the former. The same trend is also observed for the acyclic inhibitors (**2** vs **3** and **4**), although the difference is smaller. Again, the 15-membered ring **1f** is an order of magnitude more potent than the 20-membered ring **1g**. The molecular basis of the slower k_5 for **1f**−**h** is not yet clear. Another general trend is that formation of the optimal-sized macrocycle (15−17-membered) improves the overall potency of an inhibitor by 20−50-fold over their acyclic counterparts (compare **1b**−**d** vs **2**; **1f** vs **3**). We believe that the improved potency is due to the cross-linked side chain locking the inhibitor into the PDF-binding conformation.

In Vitro Antibacterial Activity. The cyclic inhibitors were first tested against *E. coli* and *Bacillus subtilis*, the representative Gram-negative and Gram-positive bacteria, respectively. For *B. subtilis*, there is a general correlation between the antibacterial activity and the K_I* values against PDF, consistent with PDF as the molecular target responsible for the observed antibacterial activity. Compounds **1b**−**d**, which are the most active inhibitors against PDF (Table 1), also exhibited the most potent antibacterial effect, with minimal inhibitory concentrations (MIC_{90} values) of 0.7−1.4, 0.2−0.4, and 0.08−0.16 μg/mL, respectively (Table 2). On the other hand, inhibitors **1a**,**e**−**g** had both poorer K_I* (3.0−36 nM) and MIC_{90} values (1.4 to >32 μg/mL). Most of the compounds were less effective against *E. coli*, and there was no correlation between the K_I* and the MIC_{90} values (Tables 1 and 2). This suggests that other factors such as efflux pumps, membrane permeability, intracellular distribution, and/or intracellular stability are at play. A notable exception is inhibitor **1f**, which is equally active against *E. coli* and *B. subtilis* (MIC_{90} = 4−8 μg/mL). Compound **1f** contains a lysine as the P_2' residue (Figure 1). It was previously reported that substitution of a P_2' lysine for a leucine substantially improved the antibacterial activity of another PDF inhibitor.[13] It is not yet clear how the inclusion of an amine group improves the cellular activity of the inhibitors.

Next, compounds **1b**,**e**,**g** were selected for testing against a panel of clinically significant pathogens including *Enterococcus faecalis*, *Haemophilus influenzae*, *Moraxella catarrhalis*, *Staphylococcus aureus*, and three *Streptococcus pneumoniae* strains. Compound **1b** had a good antibacterial activity against most of the pathogens, with MIC values ranging from 0.5 to 16 μg/mL (Table 2). The high activity of compound **1b** against *H. influenzae* strain ATCC 31517 is worth noting. This pathogen is generally difficult to treat with other antibiotics especially with the other reported PDF inhibitors.[22,37,38] To gain some insight into the molecular basis of the observed high efficacy, we tested compound **1b** against the purified *H. influenzae* PDF and found **1b** to be an exceptionally potent inhibitor against the enzyme (K_I* = 0.074 ± 0.016 nM). A K_I* value of 0.071 ± 0.007 nM was also determined for compound **1d** (against *H. influenzae* PDF). Compound **1e** had a good activity against *M. catarrhalis* and the *S. pneumoniae* strains (MIC = 0.031−8 μg/mL) but was poorly active against *E. faecalis*, *H. influenzae*, and *S. aureus* (Table 2). Compound **1g** was active only against *M. catarrhalis*, a result not unexpected from its relatively poor K_I* value.

Table 2. In Vitro Antibacterial Activity of PDF Inhibitors

bacteria	MIC_{90} (μg/mL)						
	1a	**1b**	**1c**	**1d**	**1e**	**1f**	**1g**
E. coli	>24	~12	>12	>24	>24	4−8	>32
B. subtilis	1.4−2.8	0.7−1.4	0.2−0.4	0.08−0.16	~16	~8	>32
E. faecalis (ATCC 29212)	ND[a]	>32	ND	ND	>32	ND	32
H. influenzae (ATCC 31517)	ND	0.5	ND	ND	>32	ND	32
M. catarrhalis (ATCC 37054)	ND	0.62	ND	ND	<0.031	ND	1
S. aureus (ATCC 29213)	ND	16	ND	ND	>32	ND	32
S. pneumoniae (ATCC 49619)	ND	4	ND	ND	8	ND	>32
S. pneumoniae (ATCC 6301)	ND	4	ND	ND	8	ND	>32
S. pneumoniae (ATCC 6303)	ND	2	ND	ND	4	ND	>32

[a] ND, not determined.

Table 3. Inhibition of MMPs[a]

	MMP-1 (%)		MMP2 (%)		MMP-3 (%)		MMP-9 (%)	
inhibitor	1.0 μM	10 μM	1.0 μM	10 μM	1.0 μM	10 μM	1.0 μM	10 μM
1a	0	1	10	15	3	20	8	11
1b	7	14	4	8	3	9	5	9
1e	7	8	0	0	3	4	4	6
1g	1	7	6	15	0	6	4	5
1h	3	13	17	20	0	8	8	8
3	50	100	73	98	81	99	61	94
4	50	97	34	55	68	73	54	89

[a] The values reported are the percentages of MMP activity inhibited in the presence of indicated concentrations of inhibitors. Each inhibitor was tested at two different concentrations (1.0 and 10 μM).

Cyclization Improves Inhibitor Selectivity. A major concern of any metal-chelating PDF inhibitor is its potential inhibition of the numerous metalloproteinases in the host, such as the distantly related matrix metalloproteases (MMPs). We tested several of the cyclic inhibitors (**1a**,**b**,**e**,**g**,**h**) and the acyclic controls **3** and **4** against a panel of human MMPs (MMP-1, MMP-2, MMP-3, and MMP-9). At 10 μM, the acyclic compound **3** resulted in essentially complete inhibition of all four MMPs; even at 1 μM, it caused 50−80% inhibition (Table 3). Acyclic compound **4** had a similar inhibition profile. In contrast, none of the cyclic inhibitors showed greater than 20% inhibition of MMP activity at 10 μM inhibitor concentration (Table 3). It has previously been reported that acyclic compound **2** is highly selective for PDF, showing minimal inhibition of MMPs, enkephalinase, or ACE.[21] The difference between inhibitors **2** and **3** or **4** is likely due to the presence of a bulky *tert*-butyl group at the P_2' position of **2**, which prevents binding to the active sites of these other enzymes. Remarkably, even the cyclic inhibitors that do not contain the *tert*-butyl group at the P_2' position (e.g., compounds **1g**,**h**) showed little inhibition of the MMPs. Thus, cyclization per se was sufficient to largely prevent the inhibition of MMPs. Presumably, cyclization locked the inhibitors into conformations that do not fit the active sites of these MMPs.

Cyclization Improves the Stability of Inhibitors. Inhibitors **1f** and **3** were chosen to test for the effect of cyclization on inhibitor stability. They both have an L-lysine as the P_2' residue and are expected to be sensitive to proteolytic degradation by trypsin-like enzymes. Both inhibitors were incubated in rat plasma at 37 °C, and aliquots were withdrawn at various times and analyzed by liquid chromatography−mass spectrometry (LC-MS). The cyclic inhibitor (**1f**) was very stable under the experimental conditions, showing no detectable degradation after 5 h (Figure 3). In contrast, the acyclic compound (**3**) showed time-dependent degradation, with approximately 25% loss after 5 h. Therefore, cyclization significantly improves the stability of the inhibitors against metabolic degradation. Our attempts to identify the degradation products by MS failed.

Conclusion

On the basis of earlier observations that the P_1' and P_3' side chains of PDF inhibitors are closely packed in the PDF−inhibitor complex, a new class of macrocyclic PDF inhibitors has been developed by covalently linking the two side chains. The ring size greatly affects the inhibitor properties, with 15−17-membered rings as the optimal ring size. As compared to their acyclic counterparts, the cyclic inhibitors of the optimal ring sizes show a much higher potency against PDF (>20-fold), improved stability against proteolytic degradation, and higher selectivity for PDF over other metalloproteases. To the best of our knowledge, the cyclic inhibitors rank among the most potent inhibitors reported to date against the PDF enzyme. Some of the inhibitors have good antibacterial activity against a wide spectrum of pathogens. Further development of these cyclic scaffolds may provide novel PDF inhibitors with improved metabolic stability and higher selectivity against human MMPs.

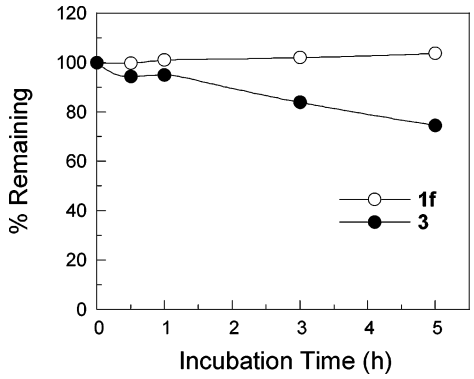

Figure 3. Comparison of the in vitro stability of PDF inhibitors **1f** (cyclic) and **3** (acyclic) in rat plasma.

Experimental Section

General. *E. coli* PDF was overexpressed and purified to apparent homogeneity with cobalt(II) as the divalent metal cofactor.[39] *H. influenzae* PDF was overproduced in *E. coli* with cobalt(II) as the metal cofactor and a C-terminal histidine tag and was purified on a cobalt(II) affinity column in a manner similar to that described for *E. coli* and *B. subtilis* PDF.[13,39] Mca-P-K-G-Dpa-A-R-NH_2 fluorogenic peptide substrate I and Mca-R-P-K-P-V-E-Nval-W-R-K(Dnp)-NH_2 fluorogenic peptide substrate II were purchased from R&D Systems (Minneapolis, MN). Cathepsin C (DPPI) and human MMPs (MMP-1, MMP-2, MMP-3, and MMP-9) were purchased from Sigma Chemical Co. (St. Louis, MO). Other chemicals were obtained from either Sigma-Aldrich (St. Louis, MO) or Bio-Rad Laboratories (Hercules, CA). Spectroscopic measurements were performed on a Perkin-Elmer Lambda 20 UV/vis spectrophotometer. Fluorogenic assays were performed with an Aminco-Bowman Series 2 Luminescence spectrometer. Molecular modeling was performed with inhibitor **1b** and was based on the crystal structure of *E. coli* PDF complexed with inhibitor **2**[21] (PDB access code 1G27) with the modeling program FLO/QXP.[40] The binding site model consisted of all protein residues within 10.0 Å of inhibitor **2**. In the binding site model, the P_1' *n*-butyl and P_3' side chains of **2** were cross-linked with polymethylene linkers of various lengths, followed by energy minimization with the peptide backbone fixed. Only the molecule with a nonyl group between the P_1' Cα carbon and the P_3' amino group was able to fit in the binding site while maintaining staggered conformations in the linker. Subsequently, the entire molecule was subjected to torsional Monte Carlo docking searches, but no lower energy binding modes were found other than the designed one.

Buffers. Buffer A: 50 mM Hepes, 10 mM NaCl, 5 mM dithiothreitol, pH 7.0. Buffer B: 100 mM Tris, 100 mM NaCl, 10 mM $CaCl_2$, 0.04% Brij-35. Buffer C: 50 mM Mops, pH 7.0.

General Procedure for the Synthesis of Aminoalkenes (8a−e). To a solution of terminal alkenol (5.0 mmol) and

triethylamine (5.5 mmol) in dichloromethane (20 mL) was added methanesulfonyl chloride (5.5 mmol) dropwise at −5 °C. The mixture was continuously stirred until the reaction was complete (∼2 h). Dichloromethane (50 mL) was added to the mixture followed by washing with 10% sodium bicarbonate solution (2 × 15 mL) and brine (15 mL). The organic layer was dried over sodium sulfate and concentrated to give the alkenyl methanesulfonyl ester in quantitative yield, which was used next without further purification. The methanesulfonyl ester (4.0 mmol) and sodium azide (10 mmol) were dissolved in 8:1 dimethyl formamide−H_2O (16 mL) and stirred overnight at 50 °C. The mixture was allowed to cool to room temperature, diluted in 50 mL of water, and extracted with diethyl ether (3 × 30 mL). The ethereal layers were combined, washed with brine (2 × 15 mL), dried over sodium sulfate, and concentrated in vacuo to give the corresponding azidoalkene. The azide (5.0 mmol) was dissolved in diethyl ether (50 mL), and lithium aluminum hydride (5.0 mmol) was added in three portions under argon in a water bath. The grayish suspension was vigorously stirred for ∼40 min and then quenched by the addition of water (5 mL). The sodium hydroxide solution was added to dissolve the solid, and the resulting solution was extracted with diethyl ether (5 × 30 mL). The organic phase was dried over sodium sulfate and concentrated to give the corresponding amines **8d**,**e**. For amines **8a**,**b**, after the $LiAlH_4$ reaction was quenched with water, Boc_2O (5.5 mmol) was added and stirred overnight. The ether layer was separated, and the residue was rinsed with ether (2 × 20 mL). The ether solutions were combined, dried over sodium sulfate, and concentrated to give the corresponding Boc-aminoalkenes. Removal of the Boc group with TFA in dichloromethane followed by exhaustive pumping gave amines **8a**,**b** as trifluoroacetate salts.

3-Butenylammonium Trifluoroacetate (8a).[41] ^{1}H NMR (250 MHz, $CDCl_3$): δ 7.53 (brs, 3H), 5.74 (m, 1H), 5.25 (m, 2H), 3.13 (m, 2H), 2.45 (m, 2H).

5-Hexenylammonium Trifluoroacetate (8b).[41] ^{1}H NMR (250 MHz, D_2O): δ 6.11−5.95 (m, 1H), 5.26−5.14 (m, 2H), 3.14 (t, J = 7.3 Hz, 2H), 2.25 (m, 2H), 1.87−1.75 (m, 2H), 1.67−1.58 (m, 2H).

7-Octenylamine (8d). ^{1}H NMR (250 MHz, $CDCl_3$): δ 5.82 (m, 1H), 4.95 (m, 2H), 2.68 (t, J = 6.8 Hz, 2H), 2.07 (m, 2H), 1.49−1.11 (m, 10H).

10-Undecenylamine (8e).[42] ^{1}H NMR (250 MHz, $CDCl_3$): δ 5.79 (m, 1H), 4.96 (m, 2H), 2.68 (t, J = 6.8 Hz, 2H), 2.03 (m, 2H), 1.53−1.04 (m, 16H).

6-Heptenylamine (8c).[43] $LiAlH_4$ (0.42 g, 11.0 mmol) and $AlCl_3$ (1.47 g, 11. 2 mmol) were added to ether (20 mL) in an ice bath. After this mixture was stirred for 5 min, a solution of 6-heptenitrile (1.00 g, 9.16 mmol) in ether (6 mL) was added dropwise and stirred until all of the nitrile was consumed. Then, 1.0 M NaOH was added to adjust the pH to ∼10 and Boc_2O (2.18 g, 10.0 mmol) was added. About 3 h later, the organic layer was separated and the aqueous layer was extracted with ether (20 mL). The ether extracts were combined and washed with water (2 × 20 mL), dried, and purified to give 1-N-Boc-6-heptenylamine (1.85 g, 95%). Removal of the Boc group with TFA gave the titled compound as its trifluoroacetate form, in quantitative yield. ^{1}H NMR (250 MHz, D_2O): δ 5.78 (m, 1H), 4.89 (m, 2H), 2.86 (t, d = 7.4 Hz, 2H), 1.97 (m, 2H), 1.54 (m, 2H), 1.37−1.18 (m, 4H).

***N*-(6-Hepten-1-yl)-L-tert-leucinamide (7c).** L-Boc-*tert*-leucine (0.65 g, 2.81 mmol) and amine **8c** (as its trifluoroacetate salt, 0.60 g, 2.64 mmol) were dissolved in a solution of dichloromethane (15 mL) and triethylamine (0.42 mL, 3.0 mmol), and then, 1-(3-dimethylaminopropyl)-3-ethylcarbodiimide hydrochloride (0.54 g, 2.82 mmol) was added. After it was stirred for about 2 h, the mixture was diluted with ethyl acetate (60 mL), washed with 5% $NaHCO_3$ (2 × 40 mL) and brine, dried over sodium sulfate, filtered, and concentrated to dryness. The residue was purified by flash chromatography to give the amide (0.75 g, 87%). ^{1}H NMR (250 MHz, $CDCl_3$): δ 6.32 (m, 1H), 5.78 (m, 1H), 5.38 (d, J = 9.5 Hz, 1H), 4.95 (m, 2H), 3.86 (d, J = 9.5 Hz, 1H), 3.28 (m, 1H), 3.16 (m, 1H), 2.03 (m, 2H), 1.53−1.27 (m, 6H), 1.43 (s, 9H), 1.00 (s, 9H). ^{13}C NMR (63 MHz, $CDCl_3$): δ 171.2, 156.3, 139.0, 114.8, 79.9, 62.7, 39.7, 34.8, 33.9, 29.8, 28.9, 28.7, 27.0, 26.8. ESI-HRMS: Calcd for $C_{18}H_{34}N_2O_3Na^+$ ([M + Na]$^+$), 349.2462; found, 349.2456. This amide (0.75 g, 2.30 mmol) was dissolved in dichloromethane (4 mL), and TFA (3 mL) was added and stirred for 2 h until all of the amide was consumed. The volatile substances were removed under vacuum. The residue was dissolved in ethyl acetate (50 mL) and was washed with 5% $NaHCO_3$ (2 × 40 mL) and brine, dried (sodium sulfate), filtered, and concentrated to give the amine (0.49 g, 94%). ^{1}H NMR (250 MHz, $CDCl_3$): δ 6.84 (m, 1H), 5.80 (m, 1H), 4.96 (m, 2H), 3.26 (m, 2H), 3.13 (brs, 1H), 2.19 (brs, 2H), 2.04 (m, 2H), 1.57−1.28 (m, 6H), 1.00 (s, 9H). ^{13}C NMR (63 MHz, $CDCl_3$): δ 173.4, 139.1, 114.8, 64.6, 39.4, 34.0, 29.9, 28.9, 27.1, 26.8. ESI-HRMS: Calcd for $C_{13}H_{26}N_2ONa^+$ ([M + Na]$^+$), 249.1937; found, 249.1950.

***N*$^\alpha$-{[(2*R*-*N*-Benzyloxy-*N*-formylamino)methyl]-6-heptenoyl}-*N*-(6-hepten-1-yl)-L-*tert*-leucinamide (5c).** This compound was prepared by coupling amine **7c** and acid **6** in a manner similar to that described for **7c** (88% yield). Compound **5c** exists as a mixture of cis and trans isomers at the formamide moiety. ^{1}H NMR (250 MHz, $CDCl_3$): δ 8.11 (brs, 0.6H), 7.86 (brs, 0.4H), 7.36 (m, 5H), 6.70 (brs, 1H), 6.61 (d, J = 9.5 Hz, 1H), 5.76 (m, 2H), 5.09−4.79 (m, 6H), 4.31 (d, J = 9.5 Hz, 1H), 3.68 (m, 1.7H), 3.36 (m, 1H), 3.08 (m, 1.3H), 2.66 (m, 0.8H), 2.43 (m, 0.2H), 2.01 (m, 4H), 1.54−1.23 (m, 10H), 0.96 (s, 9H). ^{13}C NMR (63 MHz, $CDCl_3$): δ 173.6, 170.7, 163.3, 139.0, 138.3, 134.6, 129.9, 129.5, 129.1, 115.4, 114.9, 60.9, 46.5, 45.6, 39.8, 34.8, 33.9, 30.6, 29.9, 28.9, 27.0, 26.8, 26.5. ESI-HRMS: Calcd for $C_{29}H_{45}N_3O_4Na^+$ ([M + Na]$^+$), 522.3302; found, 522.3324.

***N*-(3-*tert*-Butyl-2,5-dioxo-1,4-diaza-cyclohexadec-10-en-6-yl)methyl-*N*-benzyloxy-formamide (9c).** To a solution of alkene **5c** in dichloromethane (1.0 mM) was added 7% molar equiv of Grubb's catalyst.[30,31] The solution was stirred at 40 °C for ∼20 h, allowed to cool to room temperature, and concentrated to dryness. The residue was purified by flash chromatography to give the cyclic monomer **9c** as a mixture of cis and trans isomers at the formamide moiety (93% yield). ^{1}H NMR (250 MHz, $CDCl_3$): δ 8.10 (brs, 0.59H), 7.88 (brs, 0.41H), 7.37 (m, 5H), 6.49−6.28 (m, 2H), 5.45 (m, 0.16H), 5.34 (m, 0.84H), 5.20 (m, 1H), 4.98 (brs, 0.84H), 4.78 (brs, 1.16H), 4.28 (m, 1H), 3.79 (m, 2.66H), 3.08 (m, 0.34H), 2.83 (m, 1H), 2.57 (m, 1H), 2.11−1.78 (m, 4H), 1.55−1.03 (m, 10H), 0.94 (s, 9H). ^{13}C NMR (63 MHz, $CDCl_3$): δ 173.7, 170.9, 163.2, 134.6, 131.2, 131.1, 129.9, 129.4, 129.1, 61.1, 46.2, 39.2, 35.3, 32.8, 32.3, 30.2, 28.7, 26.9, 25.5. ESI-HRMS: Calcd for $C_{27}H_{41}N_3O_4Na^+$ ([M + Na]$^+$), 494.2989; found, 494.2972.

***N*-(3-*tert*-Butyl-2,5-dioxo-1,4-diaza-cyclohexadec-6-yl)-methyl-*N*-hydroxy-formamide (1c).** The cyclized compound **9c** (50.0 mg) was dissolved in ethyl acetate and methanol (1:1, 10 mL), and 20 mg of 10% Pd/C was added. The mixture was exposed to 1 atm of hydrogen until all of the starting material was consumed. The charcoal was removed by filtration, and the filtrate was concentrated to give the desired compound in 97% yield (as a mixture of cis and trans isomers). Reversed-phase HPLC: 99% purity. ^{1}H NMR (250 MHz, $CDCl_3$): δ 8.35 (brs, 0.23H), 7.82 (brs, 0.77H), 7.50 (d, J = 9.3 Hz, 0.23H), 7.01 (d, J = 9.1 Hz, 1H), 6.58 (m, 0.77H), 4.41 (m, 1H), 3.81 (m, 2H), 3.42 (m, 1H), 2.92−2.84 (m, 2H), 1.58−1.21 (m, 18H), 0.94 (s, 9H). ^{13}C NMR (63 MHz, $CDCl_3$): δ 173.6, 171.2, 157.5, 61.2, 53.2, 45.5, 39.5, 35.1, 30.6, 29.5, 28.0, 27.4, 27.0, 26.8, 26.4, 25.0, 24.8, 21.4. ESI-HRMS: Calcd for $C_{20}H_{37}N_3O_4Na^+$ ([M + Na]$^+$), 406.2676; found, 406.2673.

***N*-(3-*tert*-Butyl-2,5-dioxo-1,4-diaza-cyclotridec-6-yl)-methyl-*N*-hydroxy-formamide (1a).** This compound (a mixture of cis and trans isomers) was synthesized in a manner similar to **1c**. Reversed-phase HPLC: 99% purity. ^{1}H NMR (400 MHz, $CDCl_3$): δ 8.36 (brs, 0.25H), 7.85 (brs, 0.75H), 7.22 (brs, 0.42H), 6.88 (brs, 1.58H), 4.34 (d, J = 6.0 Hz, 0.25H), 4.30 (d, J = 5.3 Hz, 0.75H), 4.00 (brs, 0.25H), 3.84 (brs, 0.75H), 3.73 (m, 1H), 3.42 (m, 1H), 2.97 (m, 1H), 2.71 (m, 1H), 1.62−1.24 (m, 13H), 1.00 (s, 9H). ^{13}C NMR (100 MHz, $CDCl_3$): δ

174.5, 171.9, 157.6, 61.9, 52.2, 44.7, 39.4, 34.0, 30.0, 27.2, 26.7, 26.3, 24.4, 23.5. ESI-HRMS: Calcd for $C_{17}H_{31}N_3O_4Na^+$ ([M + Na]$^+$), 364.2207; found, 364.2207.

***N*-(3-*tert*-Butyl-2,5-dioxo-1,4-diaza-cyclopentadec-6-yl)-methyl-*N*-hydroxy-formamide (1b).** The synthesis of this compound has previously been described.[27] Reversed-phase HPLC: 96% purity.

***N*-(3-*tert*-Butyl-2,5-dioxo-1,4-diaza-cycloheptadec-6-yl)-methyl-*N*-hydroxy-formamide (1d).** This compound (a mixture of cis and trans isomers) was prepared in a manner similar to **1c**. Reversed-phase HPLC: 99% purity. ^{1}H NMR (400 MHz, $CDCl_3$): δ 9.33 (brs, 1H), 8.37 (s, 0.27H), 7.85 (s, 0.73H), 7.37 (brd, J = 8.1 Hz, 0.27H), 6.88 (brd, J = 8.1 Hz, 0.73H), 6.55 (brd, J = 6.5 Hz, 0.27H), 6.25 (brd, J = 6.5 Hz, 0.73H), 4.33 (d, J = 8.2 Hz, 1H), 3.86−3.74 (m, 2H), 3.42 (m, 1H), 2.85 (m, 2H), 1.59 (m, 2H), 1.47−1.24 (m, 18H), 0.95 (s, 9H). ^{13}C NMR (100 MHz, $CDCl_3$): δ 173.5, 171.0, 157.5, 61.2, 54.3, 53.1, 45.3, 39.0, 35.4, 32.1, 30.9, 29.7, 28.7, 28.6, 28.1, 27.4, 27.0, 25.6. ESI-HRMS: Calcd for $C_{21}H_{39}N_3O_4Na^+$ ([M + Na]$^+$), 420.2833; found, 420.2783.

***N*-(3-*tert*-Butyl-2,5-dioxo-1,4-diaza-cycloicos-6-yl)methyl-*N*-hydroxy-formamide (1e).** This compound was prepared as a mixture of cis and trans isomers (formamide) in a manner similar to **1c**. Reversed-phase HPLC: 72% purity. ^{1}H NMR (250 MHz, $CDCl_3$): δ 8.38 (brs, 0.24H), 7.83 (s, 0.7H), 8.16 (brs, 0.66H), 7.37 (s, 0.10H), 7.09 (d, J = 8.7 H, 0.23H), 6.73 (brd, J = 9.3 Hz, 0.67H), 6.14 (m, 0.23H), 6.04 (m, 0.67H), 5.93 (m, 0.1H), 4.25 (m, 1H), 4.11 (m, 0.3H), 3.81 (m, 0.7H), 3.64−3.40 (m, 2H), 2.86 (m, 1.7H), 2.72 (m, 0.3H), 1.77−1.23 (m, 26H), 1.02 (s, 2.7H), 0.97 (s, 6.3H). ^{13}C NMR (63 MHz, $CDCl_3$): δ 173.1, 170.3, 156.6, 61.1, 60.9, 51.9, 45.2, 39.6, 34.6, 30.5, 29.5, 28.9, 28.5, 27.9, 27.6, 27.5, 27.0, 26.6, 26.5, 26.0. ESI-HRMS: Calcd for $C_{24}H_{45}N_3O_4Na^+$ ([M + Na]$^+$), 462.3302; found, 462.3307.

***N*-(10-Undecen-1-yl)-N^ϵ-*tert*-butoxycarbonyl-L-lysinamide (10b).** N^α-Fmoc-N^ϵ-Boc-lysine was coupled with amine **8e** as described for **7c** to give *N*-(10-undecen-1-yl-N^α-Fmoc-N^ϵ-Boc-lysinamide in 82% yield. ^{1}H NMR (250 MHz, $CDCl_3$): δ 7.77 (d, J = 7.5 Hz, 2H), 7.59 (d, J = 7.4 Hz, 2H), 7.43−7.26 (m, 4H), 6.02 (brs, 1H), 5.82 (m, 1H), 5.44 (brs, 1H), 4.95 (m, 2H), 4.57 (brs, 1H), 4.41 (brd, J = 6.1 Hz, 2H), 4.20 (t, J = 6.8 Hz, 1H), 4.07 (m, 1H), 3.23 (m, 2H), 3.11 (m, 2H), 2.05 (m, 2H), 1.84 (m, 1H), 1.69−1.18 (m, 21H), 1.43 (s, 9H). This amide (1.86 g, 3.0 mmol) was treated with piperidine (3 mL) in dichloromethane (20 mL) for ∼40 min with stirring. The volatile solvents were removed under vacuum, and the residue was purified by silica gel chromatography to afford **10b** in 87% yield. ^{1}H NMR (250 MHz, $CDCl_3$): δ 7.26 (m, 1H), 5.83 (m, 1H), 4.97 (m, 2H), 4.55 (m, 1H), 3.29 (m, 1H), 3.23 (m, 2H), 3.12 (m, 2H), 2.04 (m, 2H), 1.83 (m, 1H), 1.60−1.28 (m, 21H), 1.44 (s, 9H). ^{13}C NMR (63 MHz, $CDCl_3$): δ 175.1, 156.4, 139.6, 114.5, 55.5, 40.5, 39.4, 35.1, 34.2, 30.4, 30.0, 29.0, 29.8, 29.7, 29.5, 29.3, 28.8, 27.3, 23.3. ESI-HRMS: Calcd for $C_{22}H_{43}N_3O_3Na^+$ ([M + Na]$^+$), 420.3197; found, 420.3174.

N^α-{[(2*R*-*N*-Benzyloxy-*N*-formylamino)methyl]-6-heptenoyl}-*N*-(10-undecen-1-yl)-N^ϵ-*tert*-butoxycarbonyl-L-lysinamide (11b). This compound was synthesized from amine **10b** and acid **6** as described for **7c** (85% yield). ^{1}H NMR (250 MHz, $CDCl_3$): δ 8.18 (brs, 0.55H), 7.83 (brs, 0.45H), 7.38 (m, 5H), 6.66 (brs, 1H), 6.54 (brs, 1H), 5.85−5.70 (m, 2H), 5.38 (brs, 0.45H), 5.03−4.77 (m, 6.55H), 4.35 (brs, 1H), 3.72 (brs, 1.45H), 3.23 (m, 2H), 3.03 (m, 2.55H), 2.58 (brs, 1H), 2.07−1.99 (m, 4H), 1.81−1.18 (m, 24H), 1.43 (s, 9H). ^{13}C NMR (100 MHz, $CDCl_3$): δ 171.7, 156.6, 139.5, 138.3, 130.1, 129.6, 129.1, 115.5, 114.5, 53.3, 40.5, 40.0, 34.2, 33.9, 29.9, 29.8, 29.6, 29.5, 29.3, 28.9, 27.3, 26.7, 22.9. ESI-HRMS: Calcd for $C_{38}H_{62}N_4O_6Na^+$ ([M + Na]$^+$), 693.4562; found, 693.4561.

***N*-{3-[4-(*tert*-Butoxycarbonylamino)butyl]-2,5-dioxo-1,4-diaza-cycloicos-10-en-6-yl}methyl-*N*-benzyloxy-formamide (12b).** This compound was synthesized from amine **11b** as described for **9c** (84% yield). ^{1}H NMR (250 MHz, $CDCl_3$): δ 8.19 (brs, 0.53H), 7.85 (brs, 0.47H), 7.39 (m, 5H), 6.40 (d, J = 8.0 Hz, 1H), 6.37 (brs, 1H), 5.32 (m, 2H), 5.01−4.60 (m, 3H), 4.30 (m, 1H), 3.73−3.43 (m, 2.5H), 3.12−2.87 (m, 3.5H), 2.53 (brs, 1H), 1.99 (m, 4H), 1.79−1.26 (m, 24H), 1.43 (s, 9H). ^{13}C NMR (63 MHz, $CDCl_3$): δ 171.6, 156.6, 131.1, 130.1, 129.6, 129.1, 53.3, 40.5, 39.6, 33.1, 31.6, 29.9, 29.4, 28.9, 28.3, 27.9, 27.6, 27.1, 26.5, 25.7, 23.0. ESI-HRMS: Calcd for $C_{36}H_{58}N_4O_6Na^+$ ([M + Na]$^+$), 665.4249; found, 665.4227.

***N*-[3-(4-Aminobutyl)-2,5-dioxo-1,4-diaza-cycloicos-6-yl]-methyl-*N*-hydroxy-formamide (1g).** Compound **12b** was hydrogenated to give the Boc-protected **1g** in quantitative yield. ^{1}H NMR (250 MHz, $CDCl_3$): δ 8.37 (brs, 0.1H), 7.76 (brs, 0.9H), 7.22 (m, 1H), 6.58 (brs, 0.1H), 6.37 (brs, 0.8H), 5.99 (brs, 0.1H), 5.08 (brs, 0.7H), 4.90 (brs, 0.1H), 4.39 (m, 1H), 3.99 (brs, 0.2H), 3.83−3.65 (m, 1H), 3.57−3.35 (m, 2H), 3.10−2.88 (m, 4.8H), 2.63 (m, 0.2H), 1.79−1.25 (m, 32H), 1.43 (m, 9H). ESI-HRMS: Calcd for $C_{29}H_{54}N_4O_6Na^+$ ([M + Na]$^+$), 577.3936; found, 577.3917. This intermediate (20 mg) was dissolved in dichloromethane (1 mL) and treated with TFA (0.5 mL). After it was stirred for 2 h at room temperature, the mixture was concentrated to dryness to give **1g**. Reversed-phase HPLC: 95% purity. ^{1}H NMR (250 MHz, CD_3OD): δ 8.32−8.26 (m, 0.4H), 7.87 (brs, 0.6H), 4.44 (m, 1H), 3.89−3.71 (m, 1H), 3.58−3.45 (m, 2H), 3.00 (m, 4H), 1.82−1.37 (m, 32H). ^{13}C NMR (63 MHz, CD_3OD): δ 176.0, 174.1, 160.4, 54.4, 46.2, 41.2, 40.9, 33.2, 31.8, 30.8, 30.3, 29.9, 29.3, 28.9, 28.6, 28.3, 28.2, 27.6, 27.5, 24.2. ESI-HRMS: Calcd for $C_{24}H_{46}N_4O_4Na^+$ ([M + Na]$^+$), 477.3411; found, 477.3410.

***N*-(5-Hexen-1-yl)-N^ϵ-*tert*-butoxycarbonyl-L-lysinamide (10a).** This compound was synthesized as described for **10b**. Amine **8b** was coupled with N^α-Fmoc-N^ϵ-Boc-L-lysine to give N^α-Fmoc-N^ϵ-Boc-lysyl (5-hexenyl)amide in 44% yield. ^{1}H NMR (250 MHz, $CDCl_3$): δ 7.71 (d, J = 7.4 Hz, 2H), 7.53 (d, J = 7.4 Hz, 2H), 7.38−7.25 (m, 4H), 6.62 (brs, 1H), 5.98 (d, J = 7.8 Hz, 1H), 5.72 (m, 1H), 4.92 (m, 2H), 4.71 (brs, 1H), 4.32 (m, 2H), 4.14 (m, 2H), 3.19 (m, 2H), 3.07 (m, 2H), 1.98 (m, 2H), 1.80−1.28 (m, 10H), 1.38 (s, 9H). ESI-HRMS: Calcd for $C_{32}H_{43}N_3O_5Na^+$ ([M + Na]$^+$), 572.3095; found, 572.3093. This amide was treated with piperidine to afford **10a** in 81% yield. ^{1}H NMR (250 MHz, $CDCl_3$): δ 7.31 (m, 1H), 5.77 (m, 1H), 4.96 (m, 2H), 4.69 (brs, 1H), 3.10 (m, 1H), 3.22 (m, 2H), 3.09 (m, 2H), 2.06 (m, 2H), 1.57 (m, 1H), 1.51−1.34 (m, 9H), 1.50 (s, 2H), 1.42 (s, 9H). ^{13}C NMR (63 MHz, $CDCl_3$): δ 175.3, 156.5, 138.6, 115.0, 79.0, 55.3, 40.4, 39.1, 34.9, 33.5, 30.1, 29.3, 28.7, 26.4, 23.2.

N^α-{[(2*R*-*N*-Benzyloxy-*N*-formylamino)methyl]-6-heptenoyl}-*N*-(5-hexen-1-yl)-N^ϵ-*tert*-butoxycarbonyl-L-lysinamide (11a). ^{1}H NMR (250 MHz, $CDCl_3$): δ 8.16 (brs, 0.56H), 7.83 (brs, 0.44H), 7.38 (m, 5H), 6.69 (m, 1H), 6.60 (brs, 1H), 5.84−5.63 (m, 2H), 5.33 (brs, 0.44H), 5.02−4.82 (m, 5.56H), 4.36 (brs, 1H), 3.87 (brs, 0.56H), 3.60 (m, 1H), 3.27−3.02 (m, 4.44H), 2.60 (m, 1H), 2.04 (m, 4H), 1.80−1.17 (m, 14H), 1.43 (s, 9H). ^{13}C NMR (63 MHz, $CDCl_3$): δ 174.1, 173.9, 171.8, 156.7, 138.7, 138.3, 130.1, 129.6, 129.1, 115.5, 115.2, 53.3, 45.4, 40.5, 39.7, 39.0, 33.8, 33.6, 29.8, 29.2, 28.9, 26.6, 26.5, 22.9. ESI-HRMS: Calcd for $C_{33}H_{52}N_4O_6Na^+$ ([M + Na]$^+$), 623.3779; found, 623.3799.

***N*-[3-(4-Aminobutyl)-2,5-dioxo-1,4-diaza-cyclopentadec-6-yl]methyl-*N*-hydroxy-formamide (1f).** This compound was prepared from **11a** in a manner similar to **1g**. Reversed-phase HPLC: 96% purity. ^{1}H NMR (400 MHz, CD_3OD): δ 8.12 (brs, 0.17H), 7.69 (brs, 0.83H), 4.25 (m, 1H), 3.71−3.27 (m, 4H), 2.82 (m, 2.83H), 2.61 (m, 0.17H), 1.55−1.11 (m, 22H). ^{13}C NMR (100 MHz, CD_3OD): δ 176.3, 174.3, 74.21, 64.7, 54.9, 46.2, 41.2, 40.1, 32.6, 30.8, 29.5, 29.1, 29.0, 28.8, 28.4, 28.3, 28.2, 26.8, 24.1. ESI-HRMS: Calcd for $C_{19}H_{36}N_4O_4Na^+$ ([M + Na]$^+$), 407.2629; found, 407.2642.

***N*-[3-(4-Acetamidobutyl)-2,5-dioxo-1,4-diaza-cyclopentadec-6-yl]methyl-*N*-hydroxy-formamide (1h).** Compound **12a** was dissolved in TFA. After concentration in vacuo, the resulting salt (9.0 mg, 13.7 μmol) was dissolved in dichloromethane (3 mL) containing triethylamine (2.1 mg, 20.6 μmol) and acetic anhydride (1.8 mg, 17.8 μmol). The product was purified by silica gel chromatography. Hydrogenation with Pd/C afforded compound **1h**. Reversed-phase HPLC: 77% purity. ^{1}H NMR (400 MHz, DMSO): δ 9.91 (s, 0.44H), 9.49 (s, 0.66H), 8.22 (s, 0.44H), 8.03 (m, 1.66H), 7.83−7.74 (m, 2H),

4.28 (m, 1H), 3.60−3.35 (m, 2H), 2.95 (m, 2H), 2.76−2.50 (m, 3H), 1.77 (s, 3H), 1.55−1.11 (m, 22H). ESI-HRMS: Calcd for $C_{21}H_{38}N_4O_5Na^+$ ([M + Na]$^+$), 449.2721; found, 449.2734.

***N*$^{\alpha}$-[(2*R*-*N*-Formyl-*N*-hydroxylamino)methyl]heptanoyl-*N*-hexyl-L-lysinamide (3).** Compound **11a** was hydrogenated on Pd/C to give Boc-protected **3** as described for **1c**. ^{1}H NMR (400 MHz, CD_3OD): δ 8.30 (s, 0.34H), 7.84 (s, 0.66H), 4.32 (m, 1H), 3.78 (m, 1H), 3.64 (dd, J = 5.5, 14.1 Hz, 0.5H), 3.45 (dd, J = 4.4, 14.1 Hz, 0.5H), 3.19 (t, J = 7.0 Hz, 2H), 3.05 (t, J = 6.6 Hz, 2H), 2.93 (m, 0.66H), 2.75 (m, 0.34H), 1.74−1.33 (m, 22H), 1.46 (s, 9H), 0.92 (m, 6H). ^{13}C NMR (100 MHz, CD_3OD): δ 174.8, 172.9, 157.5, 78.8, 53.7, 53.6, 44.8, 44.5, 40.1, 39.4, 31.9, 31.7, 30.4, 30.2, 29.5, 29.4, 27.8, 26.9, 26.7, 23.1, 22.6, 22.5, 13.4, 13.4. This resulting compound was subjected to TFA treatment to afford **3** as described for **1g**. Reversed-phase HPLC: 98% purity. ^{1}H NMR (400 MHz, CD_3OD): δ 8.19 (s, 0.19H), 7.73 (brs, 0.81H), 4.28 (m, 1H), 3.82−3.35 (m, 2H), 3.09 (m, 2H), 2.87 (m, 2.81H), 2.66 (m, 0.19), 1.69−1.21 (m, 22H), 0.82 (m, 6H). ^{13}C NMR (100 MHz, CD_3OD): δ 176.1, 174.2, 54.4, 46.1, 45.9, 41.2, 40.8, 33.3, 33.1, 33.0, 31.6, 30.8, 28.4, 28.2, 28.0, 24.2, 24.0, 23.9, 14.7. ESI-HRMS: Calcd for $C_{21}H_{42}N_4O_4Na^+$ ([M + Na]$^+$), 437.3098; found, 437.3056.

PDF Inhibition Assays. Two different assay methods were employed in this work. Method A couples the PDF reaction with AAP.[34] This assay was employed to determine the K_I* values. PDF inhibition assays were performed by incubating PDF (8 nM) in 50 mM Hepes, pH 7.0, 150 mM NaCl, 100 μM bovine serum albumin, and 0−300 nM inhibitor for 2 h on ice. The solution was brought to room temperature in a water bath, and the reaction was initiated by the addition of f-ML-pNA substrate (80 μM). After 10 min at room temperature, the reaction was quenched by heating at 95 °C for 15 min and cooled to room temperature in a water bath. AAP (1.0 unit) was added, and the resulting mixture was incubated at room temperature for 15 min. The absorbance at 405 nm was measured in a quartz cuvette on a UV/vis spectrophotometer. The background absorbance was determined by repeating the reaction but in the absence of PDF and subtracted from the observed absorbance values. The inhibition constant, K_I*, was calculated from the initial rates using the Michaelis−Menten equation: $V = (V_{max} \times [S])/\{K_M(1 + [I]/K_I^*) + [S]\}$. The percentage of substrate to product conversion was kept at <20%.

Method B couples the PDF reaction with a dipeptidyl aminopeptidase, DPPI,[36] and was employed to determine the K_I and k_6 values. Assay reactions (total volume 200 μL) were performed at room temperature in a quartz cuvette containing 5−150 μM f-Met-Lys-aminomethylcoumarin (f-Met-Lys-AMC) as the substrate, buffer A, and 0.1 U of DPPI. Prior to use, DPPI was activated by the treatment with 5 mM dithiothreitol in 50 mM Hepes (pH 7.0) and 10 mM NaCl for 30 min. The reactions were initiated by the addition of 1−10 μL (2−10 ng) of PDF and monitored continuously at 360 nm in a UV/vis spectrophotometer. The initial rates were obtained from the early part of the reaction progression curves (<30 s). The background signal was measured under the same conditions but in the absence of PDF and was subtracted from the observed PDF reaction rates. The PDF inhibition assays were performed in a similar manner except that the reactions contained 0−300 nM inhibitor and fixed concentrations of PDF (4.0 nM), DPPI (0.1 U), and f-Met-Lys-AMC (130 μM). The inhibition constant, K_I, was calculated from the initial rates using the above Michaelis−Menten equation.

To determine the rate constant, k_6, PDF (40−160 nM) and inhibitor (80−200 nM) were preincubated in 100 μL of buffer A and 100 μM BSA for 2 h on ice. The mixture was rapidly diluted into 900 μL of buffer A containing 270 μM f-Met-Lys-AMC and 0.1 U DPPI, and the reaction was monitored at 360 nm on a UV/vis spectrophotometer. After correction for background hydrolysis by DPPI, the progress curve was fitted to the equation: $Abs_{360} = V_s[t - (1 - e^{-k_6 t})/k_6]$, where V_s is the final steady state velocity. The rate constant k_5 was calculated from K_I, K_I*, and k_6 values by using the equation: $K_I^* = K_I k_6/(k_5 + k_6)$.

Inhibition of MMPs. The effect of PDF inhibitors on human MMP-1, MMP-2, MMP-3, and MMP-9 was assessed in reactions (400 μL total volume) containing buffer B, 15 μM fluorogenic MMP peptide substrate, and 0, 1, or 10 μM PDF inhibitor. For MMP-1, MMP-2, and MMP-3, peptide Mca-P-K-G-Dpa-A-R-NH_2 was employed as the substrate. For the detection of MMP-3 activity, peptide Mca-R-P-K-P-V-E-Nval-W-R-K(Dnp)-NH_2 was added to the assay. The assay reactions were initiated by the addition of 0.10 μg of the proper MMP enzyme, and the remaining MMP activity was monitored continuously on an Aminco-Bowman Series 2 luminescence spectrometer (excitation wavelength at 320 nm and emission at 405 nm).

Antimicrobial Susceptibility Testing. The antimicrobial susceptibility testing was performed using a microdilution broth assay based on the guidelines of the National Committee for Clinical Laboratory Standards (NCCLS) document M7-A5 (NCCLS, 2000). Cation-adjusted Mueller−Hinton broth (CAMHB) was used in the microtiter plates for dilution of the agent stock solution and for diluting the bacterial inoculum. For *Streptococci*, 5% lysed horse blood was added to the CAMHB. *Haemophilus* Test Medium purchased from REMEL Inc. was used for *Haemophilus* species. Inoculum was prepared by taking a sample of bacteria from a 16−20 h plate culture and adjusting it in sterile saline to an OD_{600} that corresponds to $\sim 1 \times 10^8$ colony-forming units per milliliter (CFU/mL). The saline suspension was then diluted to $\sim 1 \times 10^6$ CFU/mL in appropriate media to produce the standardized inoculum. A sample of the inoculating culture is diluted in sterile saline through a series of six 1:10 dilutions, and all dilutions are plated by spotting 10 μL of each dilution, incubated overnight at 35−37 °C, and counted the next day to verify the inoculum size.

Microtiter plates (Evergreen 96 well microplate number 222-8032-01R) were prepared with the use of the Beckman BiomekR 1000 automated laboratory workstation in combination with manual techniques. The microtiter plate was filled with 50 μL of diluent broth using the BiomekR 1000 instrument. The agent or control antibiotic stock solution was manually added to the drug well of the microtiter plate using a Calibra 852 Pipettor. The agent/antibiotic was serially diluted in 2-fold dilutions using the BiomekR 1000 instrument. Fifty microliters of the standardized bacterial inoculum was added to each well using the BiomekR 1000 instrument, producing a final inoculum of $\sim 5 \times 10^5$ CFU/mL. In addition, a nontreated growth control and commercially available control antibiotics were included to validate the assay. The final concentrations ranged from 0.03 to 32 μg/mL for test agents and 0.06 to 64 μg/mL for control antibiotics. For controls, all stock and working concentrations were 1 mg/mL. The microtiter plates were incubated overnight (16−20 h) in a 35−37 °C incubator with the exception of the *Haemophilus* and *Streptococcus* species, which were incubated at 35−37 °C and in the presence of 5% CO_2 for 24 h. The MIC_{90} is defined as the lowest concentration of agent that prevented visible growth of the organism. The end point was determined visually using a plate reading mirror.

In Vitro Stability of PDF Inhibitors in Rat Plasma. Compounds were diluted 1000-fold into rat plasma (Lot 27624, Pel-Freez, Rogers, AK) to result in an incubation concentration of 5 μg/mL. All samples were incubated at 37 °C for 0−5 h. Aliquots were withdrawn at various time points, the proteins were precipitated with acetonitrile, and internal standard was added (10 μg/mL). After the proteins were removed by centrifugation, the supernatant was analyzed for the amount of remaining parent compound by LC-MS/MS. LC was conducted on an Agilent 1100 Binary HPLC equipped with a C_{18} column. The chromatography parameters were optimized so that the analyte (**1f** and **3**) coeluted with the internal standard. MS was performed on a ThermoFinnigan LCQ-DUO instrument. MS parameters were optimized for maximal ion signal with the AutoTune routine of the Xcalibur software (ThermoFinnigan). The samples were prepared in duplicate.

Acknowledgment. We thank Professors Wim G. J. Hol and Christophe L. M. J. Verlinde (University of Washington, Seattle) for their initial computer modeling studies that suggested the feasibility of designing cyclic PDF inhibitors and Susan Hatcher (Campus Chemical Instrument Center, Ohio State University) for performing all of the mass spectrometric analysis. This work was supported by a grant from the National Institutes of Health (AI40575).

Supporting Information Available: Additional experimental details and spectral data of synthetic intermediates. This material is available free of charge via the Internet at http://pubs.acs.org.

References

(1) Giglione, C.; Pierre, M.; Meinnel, T. Peptide deformylase as a target for new generation, broad spectrum antimicrobial agents. *Mol. Microbiol.* **2000**, *36*, 1197−1205.
(2) Pei, D. Peptide deformylase: A target for novel antibiotics? *Emerging Ther. Targets* **2001**, *5*, 23−40.
(3) Yuan, Z.; Trias, J.; White, R. J. Deformylase as a novel antibacterial target. *Drug Discovery Today* **2001**, *6*, 954−961.
(4) Clements, J. M.; Ayscough, A. P.; Keavey, K.; East, S. P. Peptide deformylase inhibitors, potential for a new class of broad spectrum antibacterials. *Curr. Med. Chem. Anti-Infective Agents* **2002**, *1*, 239−249.
(5) Meinnel, T.; Mechulam, Y.; Blanquet, S. Methionine as translational start signal: A review of the enzymes of the pathway in *Escherichia coli*. *Biochimie* **1993**, *75*, 1061−1075.
(6) Mazel, D.; Pochet, S.; Marliere, P. Genetic characterization of polypeptide deformylase, a distinctive enzyme of eubacterial translation. *EMBO J.* **1994**, *13*, 914−923.
(7) Meinnel, T.; Blanquet, S. Characterization of the *Thermus thermophilus* locus encoding peptide deformylase and methionyl-tRNA(fMet) formyltransferase. *J. Bacteriol.* **1994**, *176*, 7387−7390.
(8) Margolis, P. S.; Hackbarth, C. J.; Young, D. C.; Wang, W.; Chen, D.; Yuan, Z.; White, R.; Trias, J. Peptide deformylase in *S. aureus*: Resistance to inhibition is mediated by mutations in the formyltransferase gene. *Antimicrob. Agents Chemother.* **2001**, *44*, 1825−1831.
(9) Nguyen, K. T.; Hu, X.; Colton, C.; Chakratarti, R.; Zhu, M. X.; Pei, D. Characterization of a human peptide deformylase: Implications for antibacterial drug design. *Biochemistry* **2003**, *42*, 9952−9958.
(10) Rajagopalan, P. T. R.; Yu, X. C.; Pei, D. Peptide deformylase: A new type of mononuclear iron protein. *J. Am. Chem. Soc.* **1997**, *119*, 12418−12419.
(11) Groche, D.; Becker, A.; Schlichting, I.; Kabasch, W.; Schultz, S.; Wagner, A. F. V. Isolation and crystallization of functionally competent *Escherichia coli* peptide deformylase forms containing either iron or nickel in the active site. *Biochem. Biophys. Res. Commun.* **1998**, *246*, 342−346.
(12) Meinnel, T.; Patiny, L.; Ragusa, S.; Blanquet, S. Design and synthesis of substrate analogue inhibitors of peptide deformylase. *Biochemistry* **1999**, *38*, 4287−4295.
(13) Huntington, K. M.; Yi, T.; Wei, Y.; Pei, D. Synthesis and antibacterial activity of peptide deformylase inhibitors. *Biochemistry* **2000**, *39*, 4543−4551.
(14) Wei, Y.; Yi, T.; Huntington, K. M.; Chaudhury, C.; Pei, D. Identification of a potent peptide deformylase inhibitor from a rationally designed combinatorial library. *J. Comb. Chem.* **2000**, *2*, 650−657.
(15) Chen, D. Z.; Patel, D. V.; Hackbarth, C. J.; Wang, W.; Dreyer, G.; Young, D.; Margolis, P. S.; Wu, C.; Ni, Z.-J.; Trias, J.; White, R.; Yuan, Z. Actinonin, a naturally occurring antibacterial agent, is a potent deformylase inhibitor. *Biochemistry* **2000**, *39*, 1256−1262.
(16) Apfel, C.; Banner, D. W.; Bur, D.; Dietz, M.; Hirata, T.; Hubschwerlen, C.; Locher, H.; Page, M. G. P.; Pirson, W.; Rosse, G.; Specklin, J.-L. Hydroxamic acid derivatives as potent peptide deformylase inhibitors and antibacterial agents. *J. Med. Chem.* **2000**, *43*, 2324−2331.
(17) Jayasekera, M. M. K.; Kendall, A.; Shammas, R.; Dermyer, M.; Tomala, M.; Shapiro, M. A.; Holler, T. P. Novel nonpeptidic inhibitors of peptide deformylase. *Arch. Biochem. Biophys.* **2000**, *381*, 313−316.
(18) Thorarensen, A.; Douglas, M. R., Jr.; Rohrer, D. C.; et al. Identification of novel potent hydroxamic acid inhibitors of peptidyl deformylase and the importance of the hydroxamic acid functionality on inhibition. *Bioorg. Med. Chem. Lett.* **2001**, *11*, 1355−1358.
(19) Roblin, P. M.; Hammerschlag, M. R. In vitro activity of a new antibiotic, NVP−PDF386 (VRC4887), against *Chlamydia pneumoniae*. *Antimicrob. Agents Chemother.* **2003**, *47*, 1447−1448.
(20) Coats, R. A.; Lee, S.-L.; Davis, K. A.; Patel, K. M.; Rhoads, E. K.; Howard, M. H. Stereochemical definition and chirospecific synthesis of the peptide deformylase inhibitor Sch 382583. *J. Org. Chem.* **2004**, *69*, 1734−1737.
(21) Clements, J. M.; Beckett, R. P.; Brown, A.; Catlin, G.; Lobell, M.; Palan, S.; Thomas, W.; Wittaker, M.; Wood, S.; Salama, S.; Baker, P. J.; Rodgers, H. F.; Barynin, V.; Rice, D. W.; Hunter, M. G. Antibiotic activity and characterization of BB-3497, a novel peptide deformylase inhibitor. *Antimicrob. Agents Chemother.* **2001**, *45*, 563−570.
(22) Gross, M.; Clements, J.; Beckett, R. P.; Thomas, W.; Taylor, S.; Lofland, D.; Ramanathan-Girish, S.; Garcia, M.; Difuntorum, S.; Hoch, U.; Chen, H.; Johnson, K. W. Oral anti-pneumococcal activity and pharmacokinetic profiling of a novel peptide deformylase inhibitor. *J. Antimicrob. Chemother.* **2004**, *53*, 487−493.
(23) Xue, C.-B.; He, X.; Roderick, J.; et al. Design and synthesis of cyclic inhibitors of matrix metalloproteases and TNF-α production. *J. Med. Chem.* **1998**, *41*, 1745−1748.
(24) Wei, C.-Q.; Gao, Y.; Lee, K.; et al. Macrocyclization in the design of Grb2 SH2 domain-binding ligands exhibiting high potency in whole-cell systems. *J. Med. Chem.* **2003**, *46*, 244−254.
(25) Hao, B.; Gong, W.; Rajagopalan, P. T. R.; Zhou, Y.; Pei, D.; Chan, M. K. Structural basis for the design of antibiotics targeting peptide deformylase. *Biochemistry* **1999**, *38*, 4712−4719.
(26) Guilloteau, J.-P.; Mathieu, M.; Giglione, C.; Blanc, V.; Dupuy, A.; Chevrier, M.; Gil, P.; Famechon, A.; Meinnel, T.; Mikol, V. The crystal structures of four peptide deformylases bound to the antibiotic actinonin reveal two distinct types: A platform for the structure-based design of antibacterial agents. *J. Mol. Biol.* **2002**, *320*, 951−962.
(27) Hu, X.; Nguyen, K. T.; Verlinde, C. L. M. J.; Hol, W. G. J.; Pei, D. Structure-based design of a macrocyclic inhibitor for peptide deformylase. *J. Med. Chem.* **2003**, *46*, 3771−3774.
(28) Hu, Y. J.; Wei, Y.; Zhou, Y.; Rajagopalan, P. T. R.; Pei, D. Determination of substrate specificity for peptide deformylase through the screening of a combinatorial peptide library. *Biochemistry* **1999**, *38*, 643−650.
(29) Ragusa, S.; Mouchet, P.; Lazennec, C.; Dive, V.; Meinnel, M. Substrate recognition and selectivity of peptide deformylase. Similarities and differences with metzincins and thermolysin. *J. Mol. Biol.* **1999**, *289*, 1445−1457.
(30) Miller, S. J.; Blackwell, H. E.; Grubbs, R. H. Application of ringclosing metathesis to the synthesis of rigidified amino acids and peptides. *J. Am. Chem. Soc.* **1996**, *118*, 9606−9614.
(31) Furstner, A. Olefin metathesis and beyond. *Angew. Chem., Int. Ed.* **2000**, *39*, 3012−3043.
(32) Rajagopalan, P. T. R.; Datta, A.; Pei, D. Purification, characterization, and inhibition of peptide deformylase from *Escherichia coli*. *Biochemistry* **1997**, *36*, 13910−13918.
(33) Lazennec, C.; Meinnel, T. Formate dehydrogenase-coupled spectrophotometric assay of peptide deformylase. *Anal. Biochem.* **1997**, *244*, 180−182.
(34) Wei, Y.; Pei, D. Continuous spectrophotometric assay of peptide deformylase. *Anal. Biochem.* **1997**, *250*, 29−34.
(35) Morrison, J. F.; Walsh, C. T. The behavior and significance of slow-binding enzyme inhibitors. *Adv. Enzymol.* **1988**, *61*, 201−301.
(36) Nguyen, K. T.; Hu, X.; Pei, D. Slow-binding inhibition of peptide deformylase by cyclic peptidomimetics as revealed by a new spectrophotometric assay. *Bioorg. Chem.* **2004**, *32*, 178−191.
(37) Wise, R.; Andrews, J. M.; Ashby, J. In vitro activities of peptide deformylase inhibitors against Gram-positive pathogens. *Antimicrob. Agents Chemother.* **2002**, *46*, 1117−1118.
(38) Jones, R. N.; Rhomberg, P. R. Comparative spectrum and activity of NVP-PDF386 (VRC4887), a new peptide deformylase inhibitor. *J. Antimicrob. Chemother.* **2003**, *51*, 157−161.
(39) Rajagopalan, P. T. R.; Grimme, S.; Pei, D. Characterization of cobalt(II)-substituted peptide deformylase: Function of the metal ion and the catalytic residue Glu-133. *Biochemistry* **2000**, *39*, 779−790.
(40) McMartin, C.; Bohacek, R. J. QXP: Powerful, rapid computer algorithms for structure-based drug design. *J. Comput.-Aided Mol. Des.* **1997**, *11*, 333−344.
(41) Osowska-Pacewicka, K.; Zwierzak, A. Two-carbon homologation of Grignard reagents to primary amines. *Synthesis* **1996**, *3*, 333−335.
(42) Yebassa, D.; Balakrishnan, S.; Feresenbet, E.; Raghavan, D.; Start, P. R.; Hudson, S. D. Chemically functionalized clay vinyl ester nanocomposites: effect of processing parameters. *J. Polym. Sci., Part A: Polym. Chem.* **2004**, *42*, 1310−1321.
(43) Fields, L. B.; Jacobsen, E. N. Synthesis and characterization of chiral bimetallic complexes bearing hard and soft Lewis acidic sites. *Tetrahedron: Asymmetry* **1993**, *4*, 2229−2240.

JM049592C